Photoacoustic spectral characterization of perfluorocarbon droplets

Eric Strohm[a], Ivan Gorelikov[b], Naomi Matsuura[b], Michael Kolios[a]
[a]Department of Physics, Ryerson University, Toronto, Canada;
[b]Imaging Research Department, Sunnybrook Health Sciences Centre, Toronto, Canada
mkolios@ryerson.ca

ABSTRACT

Perfluorocarbon droplets containing optical absorbing nanoparticles have been developed for use as theranostic agents (for both imaging and therapy) and as dual-mode contrast agents. Droplets can be used as photoacoustic contrast agents, vaporized via optical irradiation, then the resulting bubbles can be used as ultrasound imaging and therapeutic agents. The photoacoustic signals from micron-sized droplets containing silica coated gold nanospheres were measured using ultra-high frequencies (100-1000 MHz). The spectra of droplets embedded in a gelatin phantom were compared to a theoretical model which calculates the pressure wave from a spherical homogenous liquid undergoing thermoelastic expansion resulting from laser absorption. The location of the spectral features of the theoretical model and experimental spectra were in agreement after accounting for increases in the droplet sound speed with frequency. The agreement between experiment and model indicate that droplets (which have negligible optical absorption in the visible and infrared spectra by themselves) emitted pressure waves related to the droplet composition and size, and was independent of the physical characteristics of the optical absorbing nanoparticles. The diameter of individual droplets was calculated using three independent methods: the time domain photoacoustic signal, the time domain pulse echo ultrasound signal, and a fit to the photoacoustic model, then compared to the diameter as measured by optical microscopy. It was found the photoacoustic and ultrasound methods calculated diameters an average of 2.6% of each other, and 8.8% lower than that measured using optical microscopy. The discrepancy between the calculated diameters and the optical measurements may be due to the difficulty in resolving the droplet edges after being embedded in the translucent gelatin medium.

Keywords: Perfluorocarbon droplets, contrast agent, nanoparticles, acoustic microscopy, photoacoustic imaging, dispersion

1. INTRODUCTION

Perfluorocarbon (PFC) droplets are currently being investigated for use as ultrasound contrast agents and in cancer therapy. PFC droplets have ideal properties that make them attractive for use in medical applications; they are chemically and biologically inert[1], have high oxygen solubility and can be produced in nano- or micron-sizes for intravascular circulation[2]. PFC liquids have been investigated as blood substitute agents[3], and as contrast agents in MRI[4], and CT[5]. Upon acoustic irradiation of sufficient pressure, droplets can be vaporized using a method called acoustic droplet vaporization (ADV)[6]. The gas bubbles generated using ADV have been used as ultrasound contrast agents[6], and for cancer therapy via targeted drug delivery[7] and vessel occlusion[8].

To achieve the phase transition from liquid to gas, ADV of micron-sized droplets can require high pressures of over 8-13 MPa using 1-5 MHz [9] which may be difficult to reliably achieve in vivo. Moreover, ultrasound imaging cannot detect droplets in liquid form in the target area prior to vaporization due to their small size and poor ultrasound contrast with surrounding tissue. We have shown previously that nanoparticle-loaded nano- and micro-sized droplets can be vaporized via optical irradiation, using a method we called optical droplet vaporization (ODV)[10,11] and addresses some of the limitations associated with ADV. PFC liquids have negligible absorption in the visible and infrared optical spectrum. The optically absorbing nanoparticles loaded into droplets facilitate vaporization when irradiated with sufficient laser intensity. If an intensity less than the vaporization threshold is used, the droplet undergoes a rapid thermoelastic expansion while remaining in the liquid state, resulting in pressure wave emission. This system permits loaded droplets to be used as photoacoustic contrast agents with good contrast in comparison to the surrounding tissue, without having to vaporize the droplet. PFC nano-emulsions[12,13] and micro-emulsions[10,11] have been demonstrated as photoacoustic contrast agents. Here, we characterize the photoacoustic signals generated by the nanoparticle-loaded droplets by investigating the photoacoustic spectral response from micro-sized PFC droplets below the vaporization threshold using ultra-high frequency (over 100 MHz).

Photons Plus Ultrasound: Imaging and Sensing 2012, edited by Alexander A. Oraevsky, Lihong V. Wang,
Proc. of SPIE Vol. 8223, 82232F · © 2012 SPIE · CCC code: 1605-7422/12/$18 · doi: 10.1117/12.906042

When PFC droplets loaded with optically absorbing nanoparticles are irradiated by a laser with intensity I_0, the nanoparticles undergo rapid heating due to absorption of the optical energy. If the nanoparticles are uniformly distributed within the droplet, the entire droplet will then undergo a rapid thermoelastic expansion during laser irradiation. Assuming the droplet can be approximated by a homogenous sphere, a pressure wave at a distance r will be generated from a droplet with radius a according to

$$P(f) = i\left(\frac{\mu_a I_0 c_d \beta}{4\pi C_p (r/a)}\right) e^{-iq\tau} \frac{(\sin q - q\cos q)/q^2}{(1-\frac{\rho_d}{\rho_f})(\sin q/q) - \cos q + i\frac{c_d}{c_f}\frac{\rho_d}{\rho_f}\sin q}, \quad (1)$$

where $q = 2\pi fa/c_d$, f is the ultrasound frequency, β is the droplet thermal expansion coefficient, C_p is the droplet heat capacity, μ_a is the optical absorption coefficient of the nanoparticles within the droplet, ρ and c are the ratios of the density and sound velocity between the droplet and coupling fluid, respectively, and $\tau = (c_0/a)[t-(r-a)/c_0]$[14]. In this equation, the variables in the first bracket contribute only to the spectral amplitude, and τ and q are dimensionless time and frequency variables, respectively. This equation assumes that the physical parameters do not change as a function of frequency. For liquids where sound dispersion is present, the droplet sound speed c_d is a function of frequency, and equation 1 can be written as

$$P(f) = i\left(\frac{\mu_a I_0 c_d(f) \beta}{4\pi C_p (r/a)}\right) e^{-iq\tau} \frac{(\sin q - q\cos q)/q^2}{(1-\frac{\rho_d}{\rho_f})(\sin q/q) - \cos q + i\frac{c_d(f)}{c_f}\frac{\rho_d}{\rho_f}\sin q}, \quad (2)$$

$$\text{where} \quad q = \frac{2\pi fa}{c_d(f)}.$$

The droplet diameter is the dominant parameter that determines the frequency content of the generated photoacoustic signal and dictates the kinetics of biodistribution when injected into the bloodstream. Accurate measurement of the diameter of droplets embedded in a translucent medium to sub-micron precision using optical microscopy can be difficult; therefore the droplet diameter was calculated using ultrasound backscatter and photoacoustic methods for comparison. The droplet diameter was calculated using three independent photoacoustic and ultrasound measurements: 1) the time domain photoacoustic signal, 2) the time domain ultrasound echo from the top and bottom of the droplet, and 3) by comparing the measured photoacoustic spectrum to the model using equation 2. When a spherical droplet undergoes thermoelastic expansion upon absorption of optical energy, two forward travelling pressure waves will be emitted. The positive and negative pressure peaks create a characteristic "N-shape" in the time domain which can be used to determine the droplet diameter[15]. If the sound speed c_d in the droplet is known, then the difference in time between the positive and negative pressure peaks can be used to determine the droplet diameter using

$$d = c_d(t_2 - t_1), \quad (3)$$

where t_1 is the recorded time of the positive pressure peak and t_2 is the time of the negative pressure peak. Similarly, pulse echo methods can be used to determine the diameter of a droplet using

$$d = \frac{c_d}{2}(t_2 - t_1), \quad (4)$$

where t_1 is the echo from the top of the droplet and t_2 is the echo from the bottom of the droplet[16]. These two methods, along with the spectral comparison and direct optical imaging can be used independently to determine the droplet diameter.

2. METHOD

2.1 PFC Emulsions

Gold nanoparticles were synthesized[17], coated with silica[18], and solubilized into FC-72 (perfluorohexane)[19]. Nanoparticle-incorporated FC-72 droplets were prepared using deionized water, nanoparticle- FC-72 solution, and an anionic phosphate fluorosurfactant (Zonyl-FSP). Droplets were prepared by membrane emulsification using polymer membranes (10 μm pore size), following coarse emulsification by vortexing. Micron-scale PFC droplet size were measured using a Multisizer III Coulter counter (Beckman Coulter Inc., Fullerton, CA).

2.2 Photoacoustic Microscope

The SASAM acoustic microscope (Kibero GmbH, Germany) was used for all measurements. The microscope consists of an IX81 inverted optical microscope (Olympus, Japan) outfitted with a transducer positioned above the sample holder. The optical view allows for optical guidance during pulse echo ultrasound measurements. Photoacoustic measurements were made by collimating a 532 nm laser (Teem Photonics, France) through the back port of the microscope, which can be focused onto the sample using the same optical objective used to view the sample. The laser power was less than 30 nJ per pulse, which was low enough to avoid vaporization. This enables the microscope to be quickly switched between pulse echo or photoacoustic mode. In photoacoustic mode, the transducer is used passively to record the photoacoustic signals generated from the focused laser spot on the sample.

Transducers with a center frequency of 375 MHz (60° aperture, 42% bandwidth) and 750 MHz (100° aperture, 37% bandwidth) were used for acoustic and photoacoustic measurements. For acoustic measurements, 10 V_{pp} signals were generated by a 300 MHz monocycle pulse generator at a pulse repetition frequency (PRF) of up to 500 kHz. For photoacoustic measurements, the laser was focused onto the sample using a 10x objective (0.3 numerical aperture) and was triggered to the transducer. The transducer was aligned directly over the laser spot prior to any measurement. The laser had a pulse width of 330 ps and PRF of 4 kHz. All signals were averaged 100 times, amplified by a 40 dB amplifier (Miteq, USA) and digitized at 8 GHz. Further details on the system can be found in [11],[20].

2.3 Acoustic and Photoacoustic Measurements

All 375 MHz photoacoustic and acoustic measurements were made on droplets deposited inside gelatin phantoms approximately 200 μm thick. Droplets were added to the gelatin liquid at 37°C, then formaldehyde added to stiffen the phantom. This ensured the droplets were stabilized and could not move during experiments. Droplets close to the phantom surface were imaged to reduce attenuation losses through the gelatin. Measurements of droplets embedded in the gelatin using the 750 MHz transducer were not possible as no signal was detected due to attenuation within the gelatin. Photoacoustic measurements using the 750 MHz transducer were made with the droplets deposited on the top of a gelatin phantom. Subsequent measurements using the 375 MHz transducer were not possible as the droplets would move while switching transducers.

Droplet measurements were recorded by scanning the sample stage over a 10x10 μm area with a 0.5 μm step size. The transducer and optical objective remained stationary during scans. For pulse echo ultrasound measurements, the time of flight echoes from the top (t_1) and bottom (t_2) of the droplet were used in equation 4 to calculate the droplet diameter. For photoacoustic measurements, the time of flight of the pressure wave from the top (t_1) and bottom (t_2) of the droplet were used in equation 3 to calculate the droplet diameter. An optical image of the droplet was recorded using a CCD and compared to a microscope scale used to determine the diameter optically. Finally, the droplet diameter was found by comparing the measured droplet RF photoacoustic spectrum to the theoretical model. A fast Fourier transform (FFT) was used to obtain the spectrum from the measured RF signal generated from an individual droplet, which was then compared to the model spectrum (equation 2). A density of 1650 kg/m^3 was used for the PFC liquid, and the sound velocity was increased linearly as a function of frequency from 480 m/s at 1 MHz to 486 m/s at 1000 MHz[21]. The radius was adjusted until the spectral features (minima and maxima) between the model and measured spectrum agreed. The model gives the solution in the frequency domain, therefore an inverse FFT was used to calculate the time domain signal for direct comparison to the measured droplet signal.

The measured signals were normalized by removing the transducer response as described in reference [22]. The transducer response was found by measuring the photoacoustic signal from a 200 nm thick gold layer. A gold layer of this thickness theoretically has a flat spectrum (to within 3 dB) from 1 to 1000 MHz[23]. The spectrum measured from droplets was then divided by the measured spectrum determined from the gold film. Since the spectrum from the gold layer is nearly flat,

this photoacoustic spectrum from the gold film will give the transducer response. All measurements were windowed using a Hamming window, and a bandpass filter of 100-500 MHz for the 375 MHz transducer, and 300-1000 MHz for the 750 MHz transducer.

3. RESULTS AND DISCUSSION

3.1 Photoacoustic model and experimental comparison

The effects of sound dispersion on model accuracy were investigated using equations 1 and 2. The measured photoacoustic signal and spectrum of a 6.95 µm droplet using the 750 MHz transducer are shown in figure 1 (dashed red line). The droplet diameter was determined by adjusting the radius in equation 2 until a best fit between the model and experiment was found as discussed in section 2.3. Also shown are calculations using the model from equation 1 (solid black line, constant sound speed) and equation 2 (dotted black line, sound speed increasing from 480 m/s at 1 MHz to 486 m/s at 1000 MHz). All signals were normalized to maximum amplitude. The model was calculated in the frequency domain, and an inverse FFT used to calculate the time domain signal. For the measured signals, a FFT was used to calculate the spectrum, the transducer response removed (as described in section 2.3), filtered and windowed and the time domain signal calculated using an inverse FFT.

Both equations showed good agreement in the location of the spectral features to the measured spectrum up to 300 MHz. However at higher frequencies, the model using the variable sound speed showed better agreement to experiment using the spectral feature locations. The model using constant sound speed could not achieve a good match in the spectral feature locations over all frequencies. All further model calculations presented used equation 2 using an increasing sound speed.

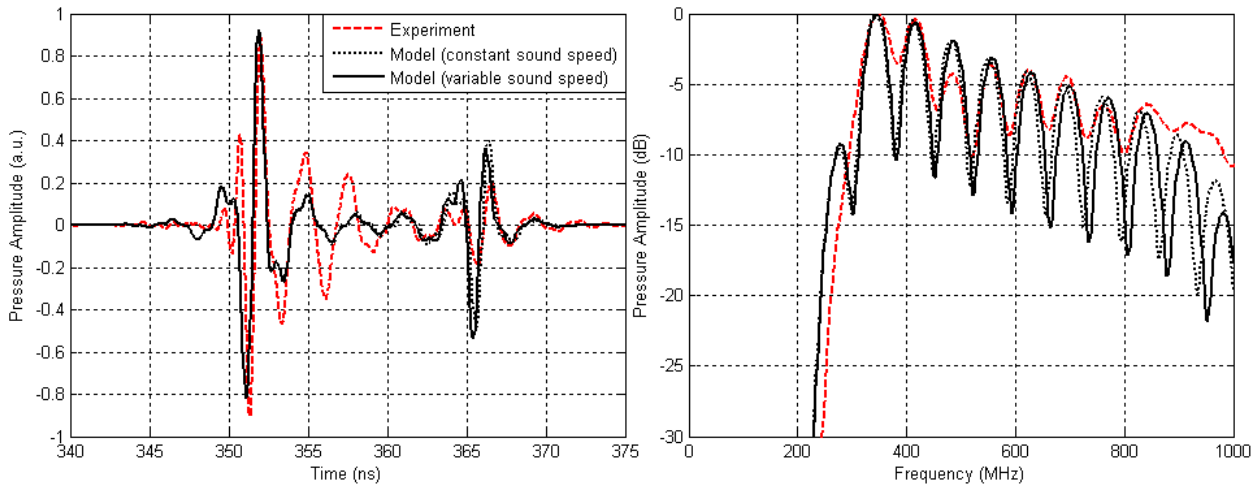

Figure 1: Photoacoustic time domain signal (left) and spectrum (right) of a 6.95 µm droplet. The droplet was measured using the 750 MHz transducer (dashed red line), while the model is shown with constant sound speed (dotted black line, equation 1) and with increasing sound speed increasing (solid black line, equation 2). The measured and both models agree well at low frequencies, however discrepancies are visible above 300 MHz due to sound speed dispersion. All signals were normalized to the maximum amplitude.

3.2 Photoacoustic measurements

The measured photoacoustic signal and spectrum of three different droplets are presented; a 5.7 µm droplet measured at 375 MHz (figure 2a and 2b), a 2.45 µm droplet measured at 750 MHz (figure 2c and 2d) and a 6.95 µm droplet measured at 750 MHz (figure 2e and 3f). All droplet diameters were determined by adjusting the radius in equation 2 until a best fit between the model and experiment was found as discussed in section 2.3. All signals were normalized to the

maximum signal amplitude. Good agreement in the location of the minima and maxima in the spectra between experiment and model was observed, as well as the location of the peaks in the time domain. The model assumes laser irradiation of a sphere composed of a homogenous liquid with uniform absorption. In this study, perfluorohexane (PFH) was used, which has negligible absorption at 532 nm. No photoacoustic signal was detected from PFH droplets without nanoparticles. However when gold nanospheres were added to the droplets, a photoacoustic signal was detected with amplitudes that varied with laser intensity. The agreement between the photoacoustic signals measured from the droplets loaded with nanoparticles and the model indicate the droplets can be modeled as a single photoacoustic source with a diameter equal to the droplet diameter, as opposed to many small photoacoustic sources from the gold nanoparticles within the droplet. The pressure wave emitted from the droplet depends primarily on the liquid parameters such as the droplet density, sound speed and diameter. The nanoparticles merely act as optical absorbers to induce a photoacoustic pressure wave. Previous measurements using lead sulphide as nanoparticles inside perfluorocarbon droplets irradiated at 1064 nm also showed good agreement between the model and spectrum[24]. This has important implications, as the data suggests that the droplets loaded with optical absorbing nanoparticles will function as a single photoacoustic source regardless of the nanoparticle type, provided the appropriate interrogating wavelength and intensity are used. However, this would likely depend on the nanoparticle concentration within the droplet. The nanoparticle concentration threshold for the droplet to behave as a single source is still unknown; this will be investigated in future experiments.

3.3 Droplet sizing

Five droplets of varying diameters were probed using both photoacoustic and pulse echo ultrasound at 375 MHz to calculate the droplet diameter to compare to the optical microscopy sizing method. Three different methods to calculate the droplet diameter were used: the time domain photoacoustic signal, the time domain ultrasound signal, and the spectral model with the diameter as an adjustable unknown parameter, and these results were compared with the droplet diameter measured directly under the optical microscope. Due to difficulties in seeing through the translucent gelatin phantom, the optical magnification was limited to the 10x objective (100x total magnification), resulting in difficulties in accurately resolving the edges of the micron-sized spherical droplets. Thus, uncertainties for the PFC droplet diameters were estimated to be ±0.5 μm.

First, the diameter was calculated from the time domain photoacoustic signal. When a transducer with infinite bandwidth is used with a delta laser pulse, the theoretical time domain signal from a droplet will have a characteristic N-shape. The theoretical photoacoustic time domain signal from a 5 μm diameter droplet is shown in figure 3a (dotted black line). The time of the first positive and negative pressure wave peaks, as shown by locations t_1 and t_2 in figure 3a, can be used to calculate the diameter of the droplet using equation 3. However the transducers used in this study have finite bandwidth, and when the theoretical N-shape response is are subjected to a Hamming window and bandpass filter of 100-500 MHz (emulating the bandpass effect of the 375 MHz transducer), the two signal peaks were observed as shown in figure 3a (solid red line). The peak locations match the start and end of the N-shape, and can therefore be used for determining the location of t_1 and t_2. Another method to determine the droplet diameter was by comparing the measured spectrum to the model spectrum. As discussed in section 2.3, the droplet diameter was adjusted until the location of the spectral features of the model and experiment agreed (see figure 2), while the sound speed and density were kept constant.

For pulse echo ultrasound measurements, the echo from the front and back of the droplet (t_1 and t_2 in figure 3b) can be used with equation 4 to calculate the droplet diameter. However this approach requires that the signal from the front and back of the droplet are separated in time, and it was found this method could not be used for droplets less than approximately 5 μm. Finally, a direct optical image was used to determine the droplet diameter. An image of the droplet was recorded by CCD, and compared to a microscope scale.

Table I summarizes the diameters using the four methods described above. Average agreement within 2.6% was found between the time domain photoacoustic and ultrasound methods and the photoacoustic model method. The optical sizing method was found to be an average 8.8% higher than the other three methods. The discrepancy between the optical and signal-based measurements could be due to the difficulty in optically observing the droplets through a partially translucent gelatin medium, which limited observation to the 10x objective. The estimation of droplet size from the model using equation 2 was similar to the photoacoustic and ultrasonic time domain methods (difference less than 3%). Therefore the droplet diameter determined from the model comparison was reported as the actual diameter instead of the optical sizing method in sections 3.1 and 3.2.

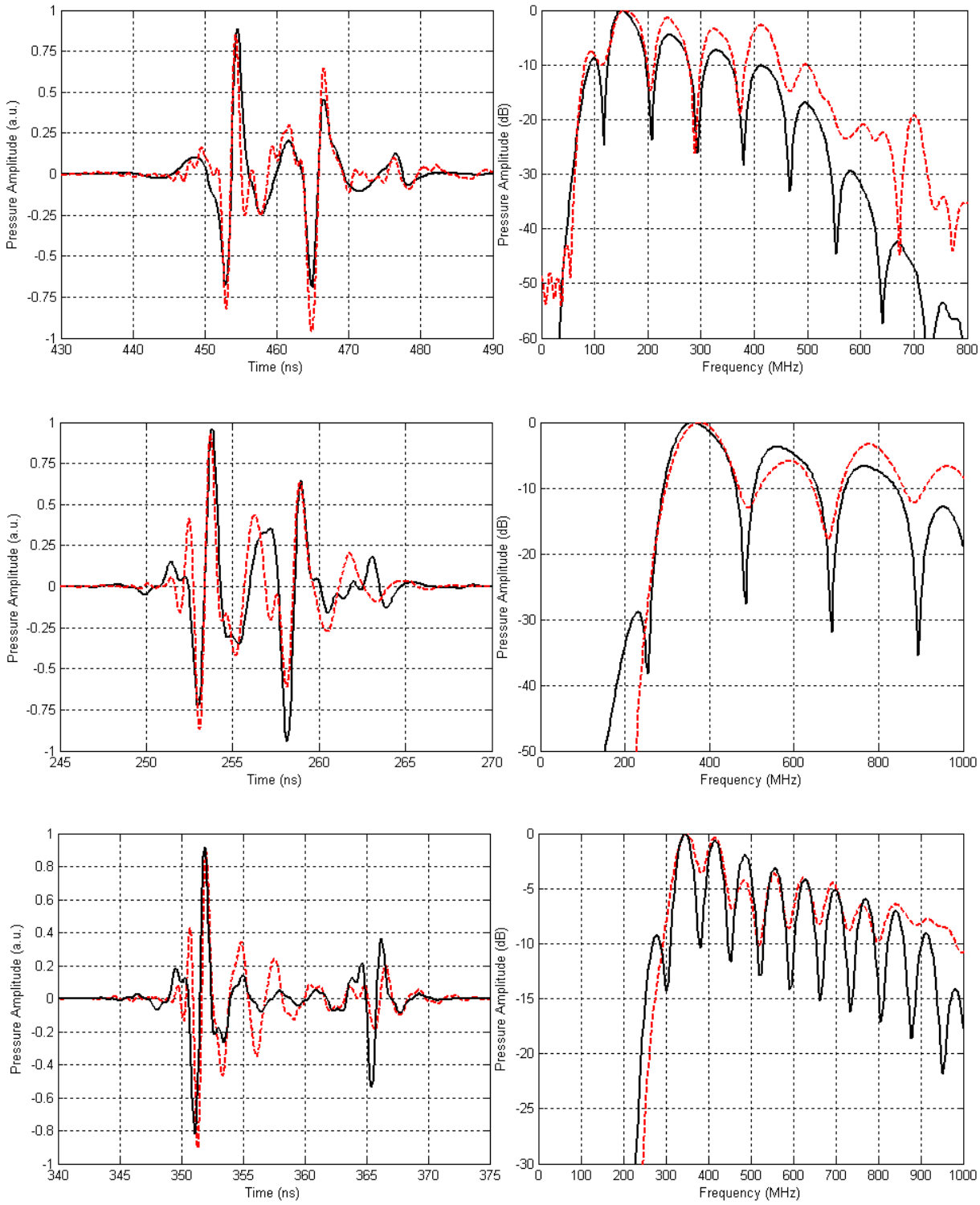

Figure 2: The measured photoacoustic time domain signal (left) and spectrum (right) from three different droplets (red dashed line), compared to the model (equation 2, solid black line). A 5.7 µm droplet measured at 375 MHz (top), a 2.45 µm droplet measured at 750 MHz (middle), and a 6.95 µm droplet measured at 750 MHz (bottom). Good agreement in the location of the spectral features between experiment and model were observed. All signals were normalized to maximum amplitude.

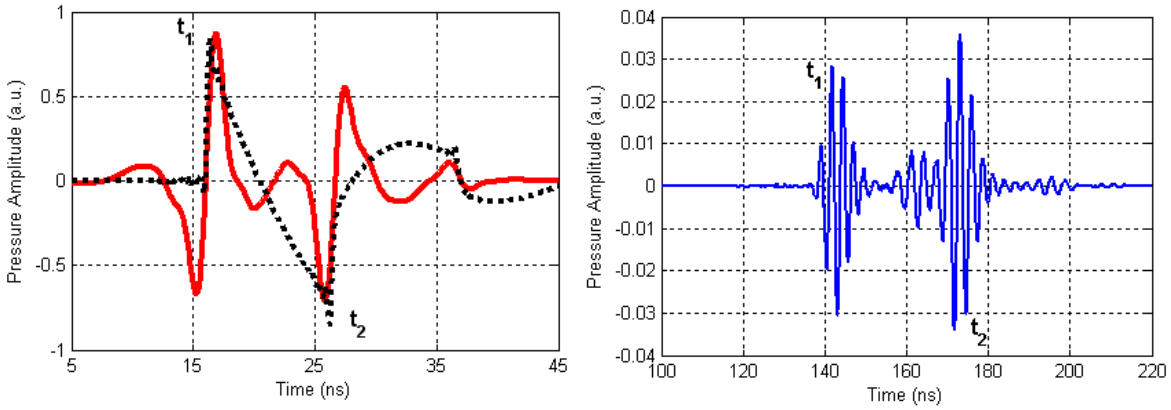

Figure 3: Left: The theoretical photoacoustic time domain signal of a 5 μm droplet from equation 2 (dotted black line) and using a Hamming window with a bandpass filter of 100-500 MHz emulating the 375 MHz transducer (solid red line). Right: The measured ultrasound echo from a 7.2 μm diameter droplet embedded in gelatin. The labels t_1 and t_2 were used to calculate the droplet diameter using equation 3 (photoacoustic signal, left) and equation 4 (ultrasound signal, right).

Table 1. Calculation of the droplet diameter using the photoacoustic signal and equation 3, the ultrasound signal and equation 4, experimental and model spectral comparison (equation 2) and direct optical measurement. The diameter of droplet #2 could not be calculated using ultrasound methods as the signals overlapped.

Droplet Number	Droplet Diameter (μm)			
	Photoacoustic	Ultrasound	Model	Optical
1	6.86	6.98	6.95	7.40
2	4.68	-	4.90	5.14
3	5.04	5.16	5.40	5.70
4	7.97	8.06	8.10	9.14
5	7.10	7.06	7.20	8.00

4. CONCLUSIONS

The photoacoustic spectra from single micron sized droplets were shown to agree with a theoretical model that assumes a homogenous optical absorbing spherical liquid, and the agreement was improved when the model accounted for changes in sound speed as a function of frequency. Since the model assumes a homogenous uniformly irradiated sphere that undergoes thermoelastic expansion, we can conclude that the nanoparticle-loaded droplet can be modeled as a single photoacoustic source emitting a pressure wave that depends on the PFC liquid properties, and not those of the nanoparticles. In addition, four independent methods used to calculate the droplet diameter were found to agree. In particular, the method using the time domain photoacoustic signal, time domain ultrasound signal and the photoacoustic model fit agreed to each other within 2.6%, while the droplet diameter using the direct optical measurement was 8.8% higher. The larger errors associated with the optical measurement may be due to difficulty in determining the droplet borders when embedded in an optically translucent medium.

5. ACKNOWLEDGEMENTS

E. Strohm is supported through a NSERC doctoral scholarship. This research was undertaken, in part, thanks to funding from NSERC and the Canada Research Chairs Program awarded to M. Kolios. Funding to purchase the equipment was provided by the Canada Foundation for Innovation, the Ontario Ministry of Research and Innovation, and Ryerson University. This study was supported, in part, by the Ontario Institute for Cancer Research Network through funding provided by the Province of Ontario, the FY07 Department of Defense Breast Cancer Research Program Concept Award (BC075873), a program project grant entitled “Imaging for Cancer” from the Terry Fox Foundation, and the Ontario Research Fund-Research for Excellence Program.

REFERENCES

[1] Cohn, C.S., and Cushing, M.M., "Oxygen therapeutics: perfluorocarbons and blood substitute safety," Crit. Care Clin. 25(2), 399-414 (2009).

[2] Fast, J.P., and Mecozzi, S., [Nanoemulsions for Intravenous Drug Delivery], in Nanotechnology in Drug Delivery, M. M. Villiers, P. Aramwit, and G. S. Kwon, Eds., Springer New York, New York, NY, 461-489 (2009).

[3] Riess, J.G., and LeBlanc, M., "Solubility and transport phenomena in perfluorochemicals relevant to blood substitution and other biomedical applications," Pure Appl. Chem. 54(12), 2383-2406 (1982).

[4] Mattrey, R.F., Hajek, P.C., Gylys-Morin, V.M., Baker, L.L., Martin, J., Long, D.C., and Long, D.M., "Perfluorochemicals as gastrointestinal contrast agents for MR imaging: preliminary studies in rats and humans," Am. J. Roentegenol. 148(6), 1259-63 (1987).

[5] Behan, M., O'Connell, D., Mattrey, R.F., and Carney, D.N., "Perfluorooctylbromide as a contrast agent for CT and sonography: preliminary clinical results," Am. J. Roentegenol. 160(2), 399-405 (1993).

[6] Kripfgans, O.D., Fowlkes, J.B., Miller, D.L., Eldevik, O.P., and Carson, P.L., "Acoustic droplet vaporization for therapeutic and diagnostic applications," Ultrasound in Med. & Biol. 26(7), 1177-1189 (2000).

[7] Fabiilli, M.L., Haworth, K.J., Sebastian, I.E., Kripfgans, O.D., Carson, P.L., and Fowlkes, J.B., "Delivery of chlorambucil using an acoustically-triggered perfluoropentane emulsion," Ultrasound in Med. & Biol. 36(8), 1364-75 (2010).

[8] Kripfgans, O.D., Fowlkes, J.B., Woydt, M., Eldevik, O.P., and Carson, P.L., "In vivo droplet vaporization for occlusion therapy and phase aberration correction," IEEE Trans. Ultrason., Ferroelectr., Freq. Control 49(2), 726-738 (2002).

[9] Zhang, M., Fabiilli, M.L., Haworth, K.J., Fowlkes, J.B., Kripfgans, O.D., Roberts, W.W., Ives, K. a, and Carson, P.L., "Initial investigation of acoustic droplet vaporization for occlusion in canine kidney," Ultrasound in Med. & Biol. 36(10), 1691-703 (2010).

[10] Strohm, E.M., Kolios, M.C., Gorelikov, I., and Matsuura, N., "Optical Droplet Vaporization (ODV): photoacoustic characterization of perfluorocarbon droplets," in IEEE Ultrasonics Symposium (2010).

[11] Strohm, E., Rui, M., Gorelikov, I., Matsuura, N., and Kolios, M., "Vaporization of perfluorocarbon droplets using optical irradiation," Biomedical Optics Express 2(6), 1432-1442 (2011).

[12] Wilson, K.E., Homan, K.A., and Emelianov, S.Y., "Remotely Triggered Contrast NanoAgent for Ultrasound and Photoacoustic Imaging," in IEEE Ultrasonics Symposium, 1003-1006 (2010).

[13] Wilson, K., Homan, K., and Emelianov, S., "Photoacoustic and ultrasound imaging contrast enhancement using a dual contrast agent," in Proc. SPIE 7564, 75642P-75642P-5 (2010).

[14] Diebold, G.J., Sun, T., and Khan, M.I., "Photoacoustic monopole radiation in one, two, and three dimensions," Phys. Rev. Lett. 67(24), 3384-3387 (1991).

[15] Diebold, G.J., Khan, M.I., and Park, S.M., "Photoacoustic 'Signatures' of Particulate Matter: Optical Production of Acoustic Monopole Radiation," Science 250(4977), 101-104 (1990).

[16] Briggs, A., and Kolosov, O., [Acoustic microscopy], Oxford University Press, USA (2009).

[17] Bastús, N.G., Comenge, J., and Puntes, V., "Kinetically Controlled Seeded Growth Synthesis of Citrate-Stabilized Gold Nanoparticles of up to 200 nm: Size Focusing versus Ostwald Ripening," Langmuir 27(17), 11098-11105 (2011).

[18] Liz-Marzán, L.M., Giersig, M., and Mulvaney, P., "Synthesis of Nanosized Gold−Silica Core−Shell Particles," Langmuir 12(18), 4329-4335 (1996).

[19] Gorelikov, I., Martin, A.L., Seo, M., and Matsuura, N., "Silica-Coated Quantum Dots for Optical Evaluation of Perfluorocarbon Droplet Interactions with Cells," Langmuir 27(24), 15024-15033 (2011).

[20] Strohm, E.M., Czarnota, G.J., and Kolios, M.C., "Quantitative measurements of apoptotic cell properties using acoustic microscopy," IEEE Trans. Ultrason., Ferroelectr., Freq. Control 57(10), 2293-2304 (2010).

[21] Strohm, E.M., and Kolios, M.C., "Sound velocity and attenuation measurements of perfluorocarbon liquids using photoacoustic methods," in IEEE Ultrasonics Symposium (2011).

[22] Baddour, R.E., Sherar, M.D., Hunt, J.W., Czarnota, G.J., and Kolios, M.C., "High-frequency ultrasound scattering from microspheres and single cells," J. Acoust. Soc. Am. 117(2), 934 (2005).

[23] Khan, M., Sun, T., and Diebold, G., "Photoacoustic waves generated by absorption of laser radiation in optically thin layers," The Journal of the Acoustical Society of America 93(3), 1417 (1993).

[24] Strohm, E.M., Rui, M., Gorelikov, I., Matsuura, N., and Kolios, M., "Optical Droplet Vaporization of Micron-sized Perfluorocarbon Droplets and their Photoacoustic Detection," in Proc. SPIE, 78993H-1-78993H-7 (2011).